SUPPLEMENTARY INFORMATION

Differential kinase activity across prostate tumor compartments defines sensitivity to target inhibition

Running Title: Differential kinase activity across tumor compartments

Nezihi Murat Karabacak[*1,2], Yu Zheng[*3], Taronish D. Dubash[3], Risa Burr[3], Douglas S. Micalizzi[3], Ben S. Wittner[3], Maoxuan Lin[3], Devon Wiley[3], Valentine Comaills[3], Erin Emmons[3], Kira Niederhoffer[3], Uyen Ho[3], Jacob Ukleja[3], Dante Che[3], Hannah Stowe[1,2], Linda Nieman[3], Wilhelm Haas[3], Shannon L. Stott[3], Michael S. Lawrence[3], David T. Ting[3], David T. Miyamoto[3], Daniel A. Haber[3,4], Mehmet Toner[1,2], Shyamala Maheswaran[3, 5]

[1] Center for Engineering in Medicine and Surgery, Massachusetts General Hospital, Harvard Medical School

[2]Shriners Hospital for Children, Boston, MA 02114.

[3]Massachusetts General Hospital Center for Cancer Research, Harvard Medical School, Charlestown, MA 02129.

[4]Howard Hughes Medical Institute, Bethesda, MD, 20815.

Supplementary Figure 1

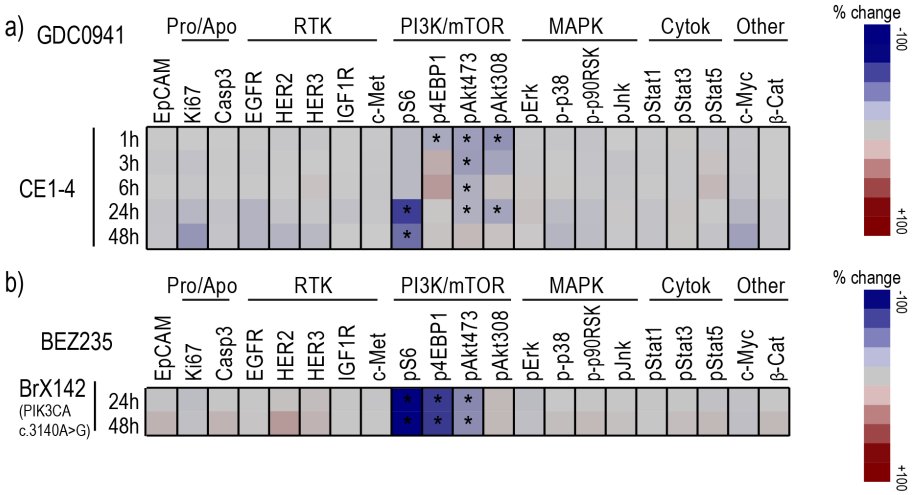

Supplementary Figure 1:

1a: Heatmap showing mean change in the signaling proteins within each of the indicated pathways in CE1-4 cells treated *in vitro* with the PI3K inhibitor, GDC0941, compared with untreated control cells (n=2 experimental replicates). Significant changes are marked with asterisks. $p<0.01$ corrected for multiple comparisons by Bonferroni-Dunn.

1b: Heatmap showing mean changes in proteins following BEZ235 treatment of the breast cancer patient derived PI3K mutant CTC cell line, BRX142. $p<0.01$ corrected for multiple comparisons by Bonferroni-Dunn.

Supplementary Figure 2

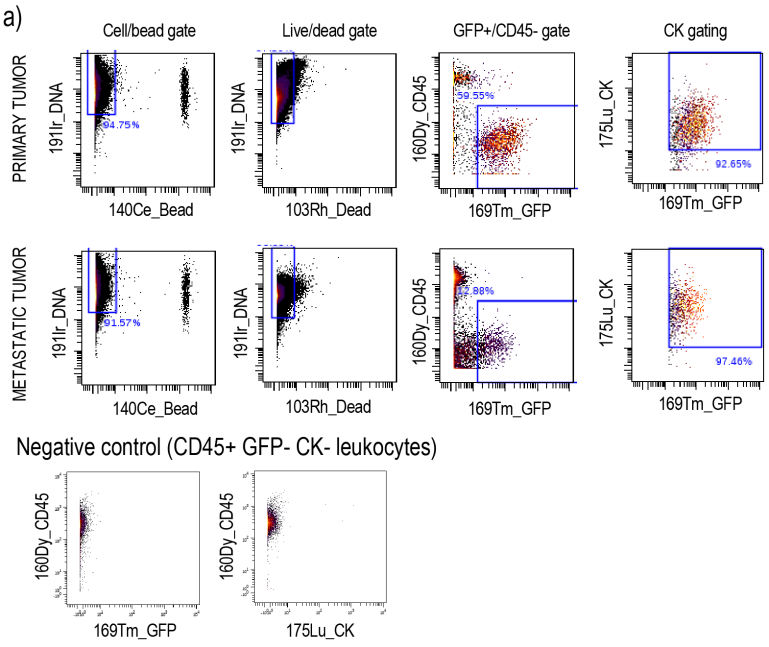

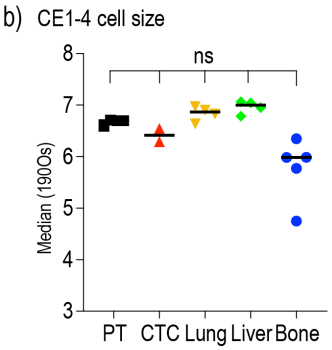

Supplementary Figure 2:

2a: Gating strategy used for selecting tumor cells from mass cytometry data of mouse prostate cancer graft models. We performed manual gating of events positive for nucleic acid intercalator, CK, GFP and negative for CD45, Ce140 (control bead). Top and middle series of panels show cells from primary and metastatic PC3 tumors, bottom panel shows leukocytes.

2b: Osmium tetroxide labeling applied to the CE1-4 tumor model to compare cell sizes across the different tumor sites shows no significant differences (PT: Primary tumor, ns: not significant) ($p=0.2301$ for PT vs Bone, $p=0.2441$ for PT vs Liver, $p=0.4637$ for PT vs Lung, $p=0.4637$ for PT vs CTC).

Supplementary Figure 3

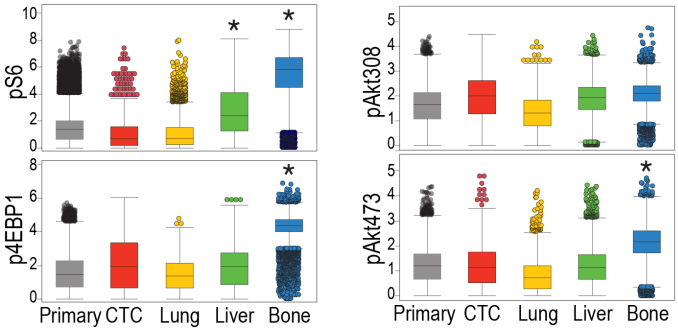

Supplementary Figure 3:

Box and whisker plots showing signals from individual epitopes used to generate the PI3K/mTOR score in PC3 cells (* indicates $p<0.01$).

Supplementary Figure 4

a)

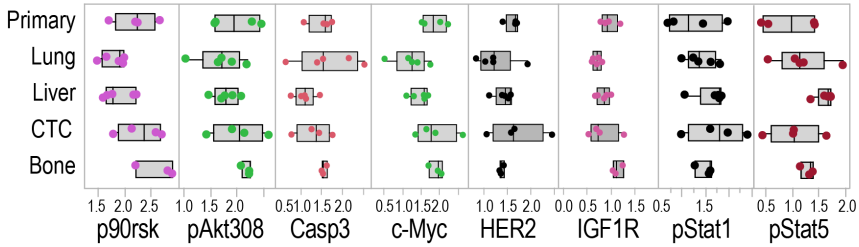

b)

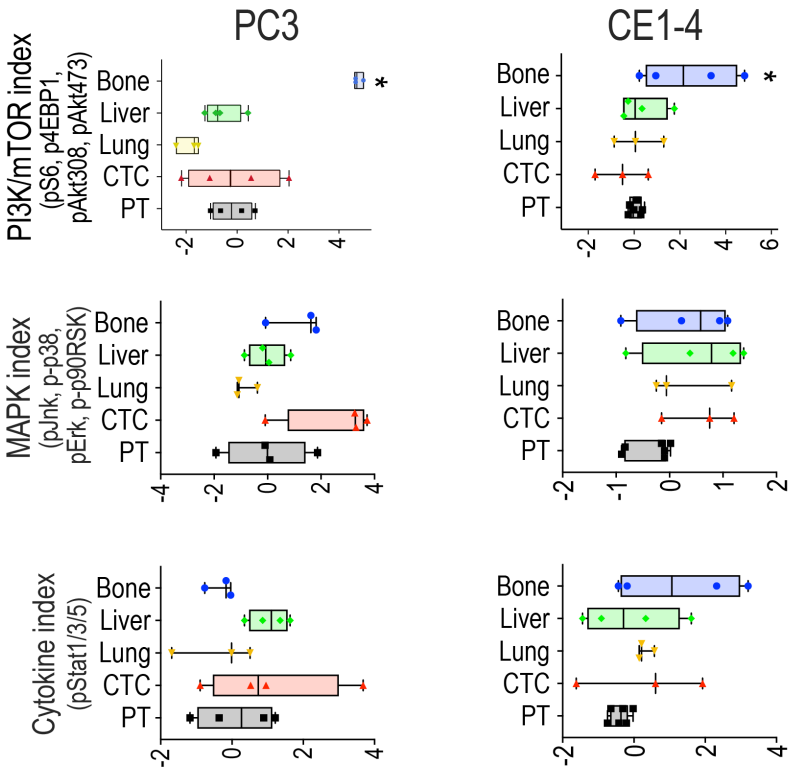

Supplementary Figure 4:

a) Plots showing median signal of epitopes that were not significantly different across PC3 tumor deposits at different sites.

b) PI3K/mTOR, MAPK and cytokine pathway signatures show median levels of each of the pathways in primary and metastatic tumor cells and in CTCs in PC3 and CE1-4 models. These signatures were calculated by summing standardized levels of epitopes shown in y axes. Pathways significantly elevated are marked with asterisks. $q<0.1$, one-way ANOVA, FDR correction.

Supplementary Figure 5

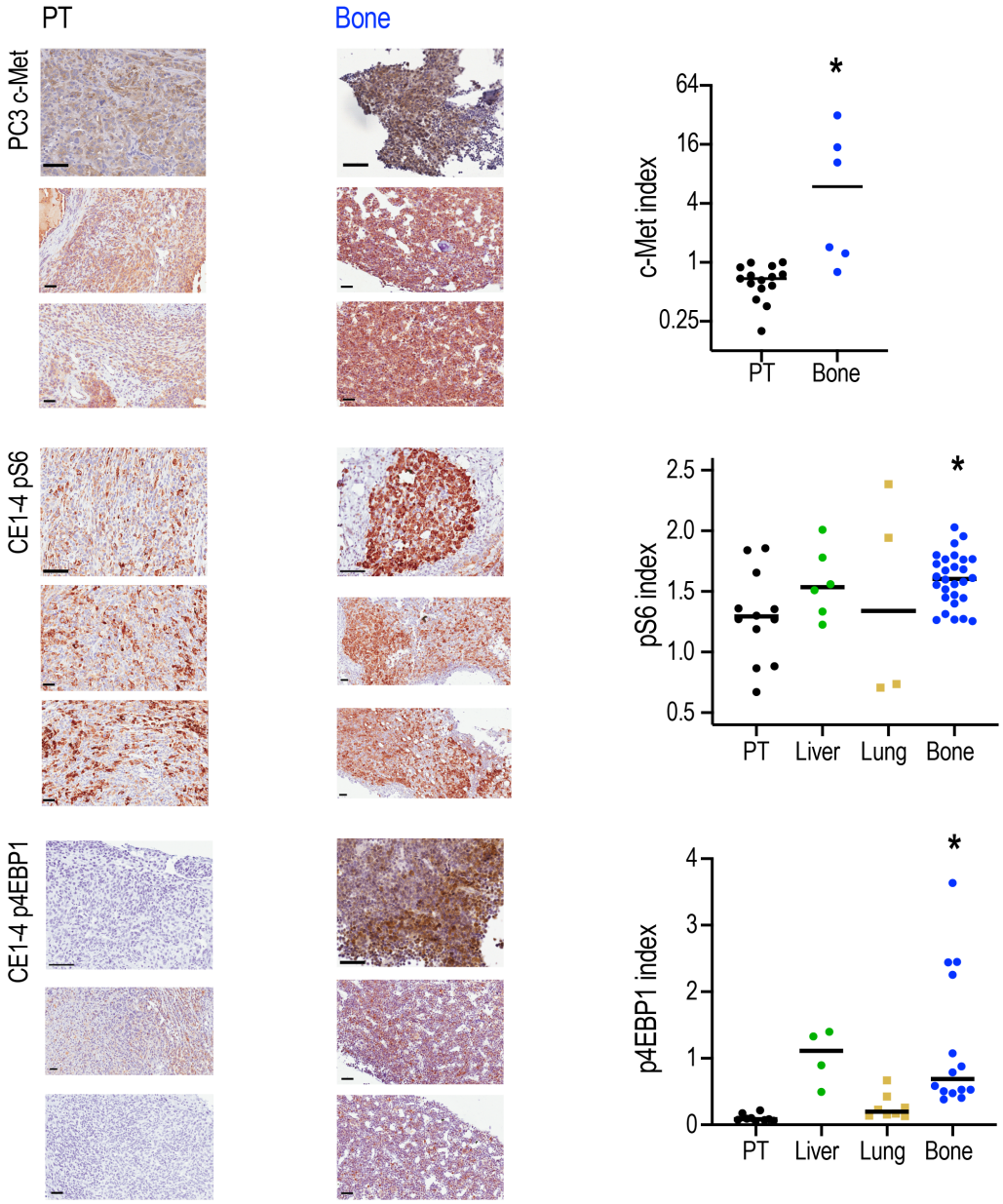

Supplementary Figure 5:

The primary tumors and bone metastases derived from the graft models shown were stained for c-Met, pS6 or p4EBP1 (DAB) and counterstained with hematoxylin. Representative images are shown (left). Scale bars represent 50 µm. Quantification of c-Met, pS6 and p4EBP1 levels show significantly increased expression for all three epitopes in bone metastases when compared to primary tumors (right panels). c-Met: p=0.0182 by Mann-Whitney test, pS6: p=0.0386, and p4EBP1 p=0.0019 by one-way ANOVA, Holm-Sidak's multiple comparisons test.

Supplementary Figure 6

MET gene in human prostate cancer

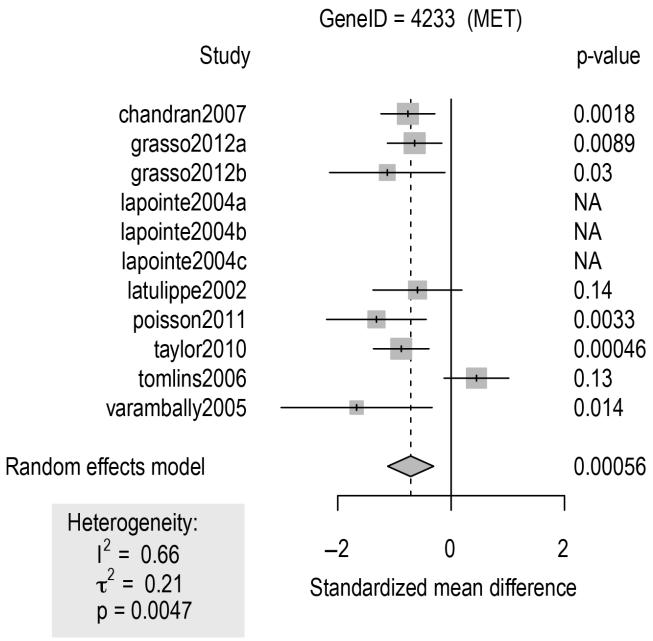

Supplementary Figure 6:

Meta-analysis of c-Met gene expression in prostate cancer datasets that have both primary and metastatic tumors. Data shows significantly reduced c-Met mRNA expression in metastatic tumors.

Supplementary Figure 7

Human Prostate Cancer c-Met IHC

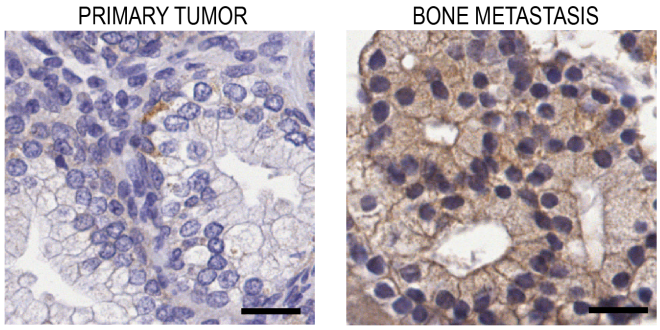

Supplementary Figure 7:

c-Met protein expression in the primary tumor and in bone metastasis derived from human prostate cancer patients was measured using IHC. Representative images of c-Met and hematoxylin counter-stained primary tumors and bone metastases are shown. Scale bar represents 50μm. The quantification of c-Met index showed elevated c-Met protein levels in bone metastases compared with primary tumors (**Fig. 2g**).

Supplementary Figure 8

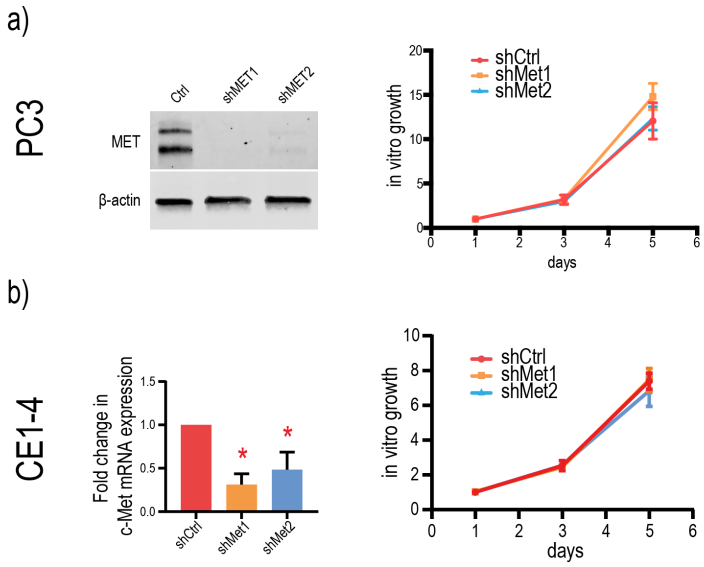

Supplementary Figure 8:

8a: Knockdown of c-Met expression in PC3 cells using two different shRNAs against c-Met. Depletion of c-Met protein in PC3 cells is shown. ß-actin is shown as loading control. The plot on the right shows that c-Met knockdown does not impair cell proliferation *in vitro*. q=0.8654 CTR vs shMET1, q=0.9553 CTR vs shMET2 by two-way ANOVA, FDR correction.

8b: Knockdown of c-Met expression in CE1-4 cells using two different shRNAs against c-Met shows reduced expression c-Met RNA ($p<0.01$, t-test). c-Met-KD does not interfere with *in vitro* proliferation. q=0.8999 CTR vs shMET1, q=0.5529 CTR vs shMET2, two-way ANOVA, FDR correction.

Supplementary Figure 9

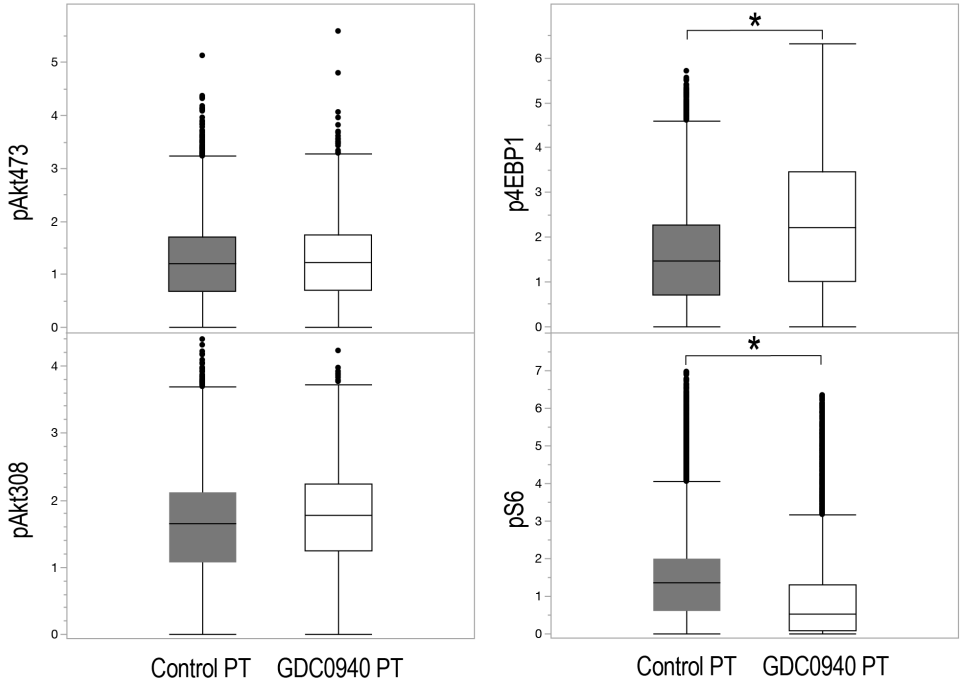

Supplementary Figure 9:

Box and whisker plots showing signals from individual epitopes used to generate the PI3K/mTOR score in GDC0941 treated PC3 dataset (* indicates $p<0.01$).

Supplementary Figure 10

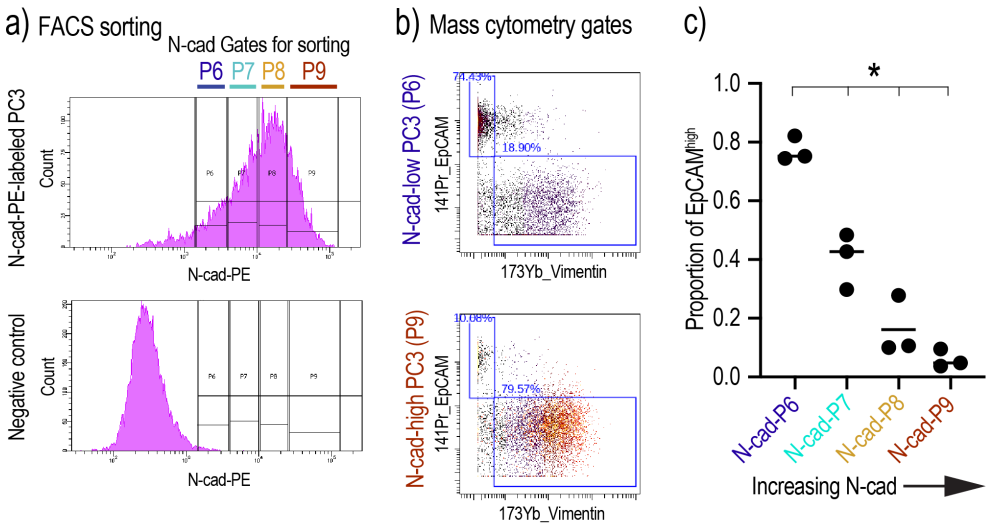

Supplementary Figure 10:

10a: PC3 cells, grown *in vitro*, were sorted into 4 populations based on their level of N-Cadherin (N-Cad) expression, labeled as P6, P7, P8 and P9, from lowest to highest N-Cad, respectively. Top panel shows the level of N-Cad detected in sorted cells via PE fluorescence intensity. Bottom panel; trypsin treated N-Cad cells that lost the N-Cad epitope are shown as negative control.

10b: Gating strategy for analysis of $EpCAM^{high}$ cell proportion in N-Cad sorted PC3 cells, top panel showing P6 ($N\text{-}Cad^{low}$) and bottom panel showing P9 ($N\text{-}Cad^{high}$). Top left quadrant was used to quantify $EpCAM^{high}$ cells.

10c: Proportion of $EpCAM^{high}$ cells compared within sorted populations. Proportion of $EpCAM^{high}$ PC3 population significantly decreases with increasing N-Cad levels. q=0.0207 N-cad-P6 vs N-cad-P7, q=0.0207 N-cad-P6 vs N-cad-P8, q=0.0087 for N-cad-P6 vs N-cad-P9, one-way ANOVA, FDR correction.

Supplementary Figure 11

Prostate cancer CTC dataset (13 patients, 77 CTCs)

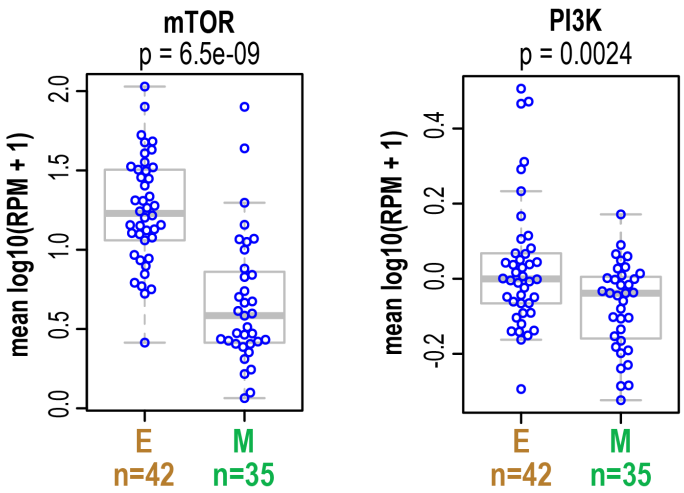

Supplementary Figure 11:

Epithelial and mesenchymal prostate cancer CTC subsets were defined based on single cell RNA sequencing data and analyzed for mTOR and PI3K signatures. The p-values shown were calculated using the two-sided Welch t-test.

Supplementary Figure 12

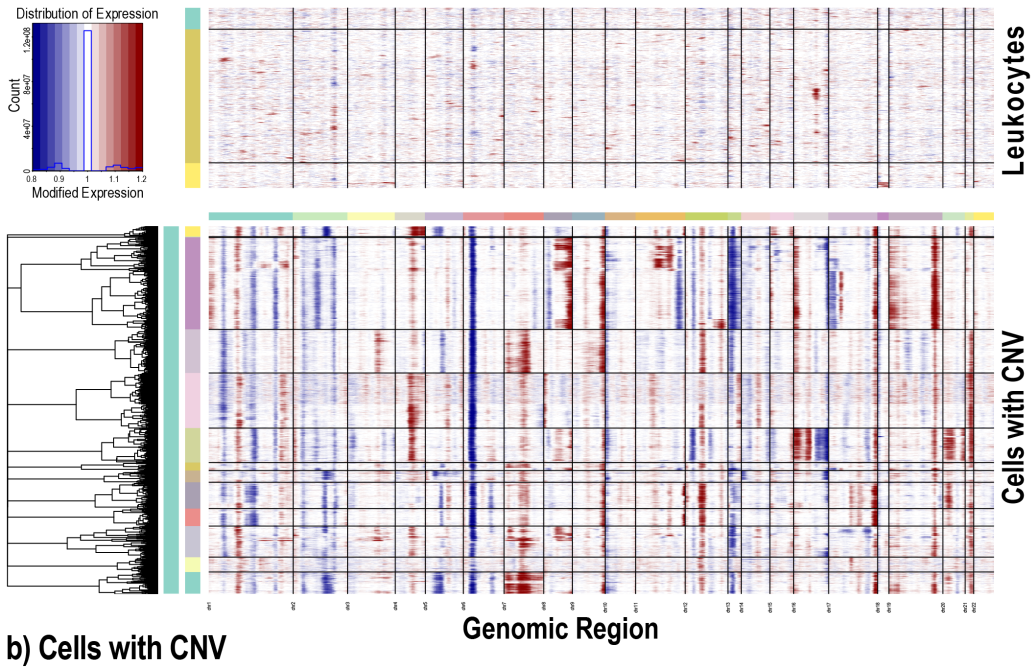

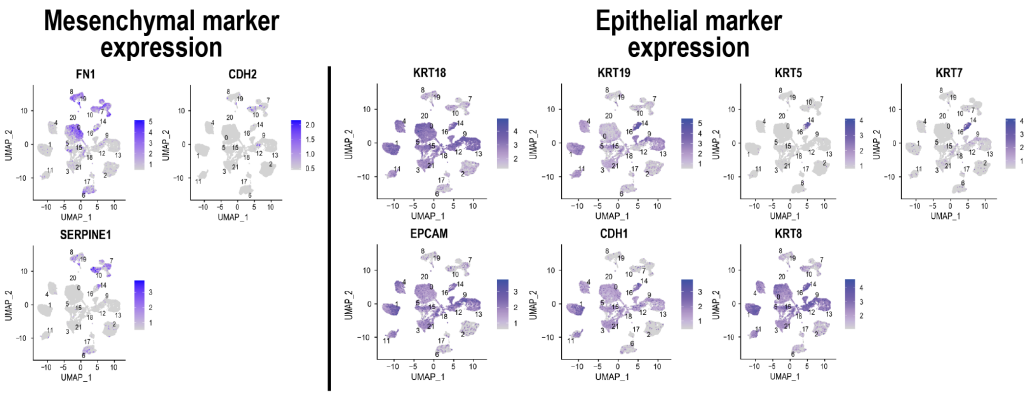

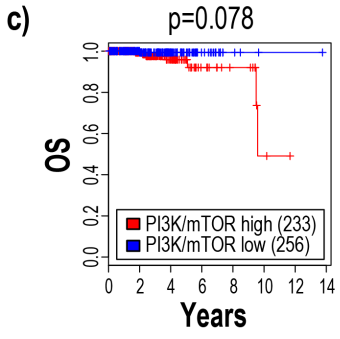

Supplementary Figure 12:

12a: Identification of tumor cells via inferCNV analysis. Top panel shows leukocytes that were used as reference and bottom panel shows CNV-positive putative tumor cells.

12b: UMAP plots showing mesenchymal and epithelial marker expression in clustered cells with CNV. Cell with CNVs were separated into E/M subpopulations and used for the PI3K/mTOR analysis in Figure 5d.

12c: Kaplan-Meier analysis of overall survival (OS) upon analysis of TCGA-PRAD transcriptome data from prostate cancer patients shows that high average PI3K/mTOR activity trends toward predicting poor overall survival. The high and low PI3K/mTOR subgroups were determined based on average PI3K/mTOR activity using Otsu's method(1). P-value was calculated by log rank test.

Supplementary Figure 13

a) Breast cancer CTC dataset 1 (45 patients, 135 CTCs)

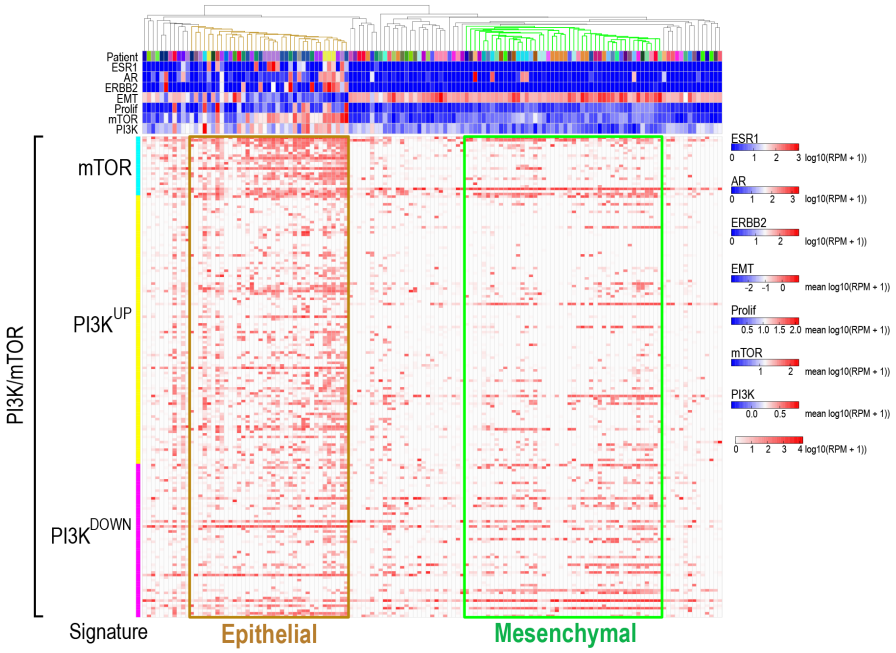

b)

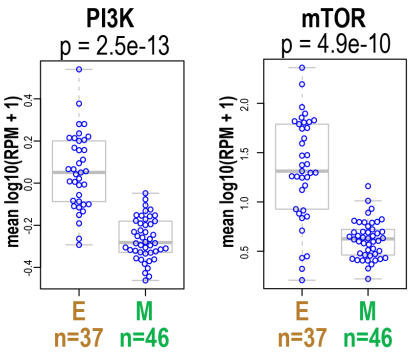

Supplementary Figure 13:

The plots show the level of the individual PI3K and mTOR signaling and combined PI3K/mTOR gene signatures in each individual CTCs enriched from breast cancer patients (dataset #1) harboring wild type or mutant PI3K. The p-values shown were calculated using the two-sided Welch t-test.

Supplementary Figure 14

a) Breast cancer CTC dataset 2 (33 patients, 106 CTCs)

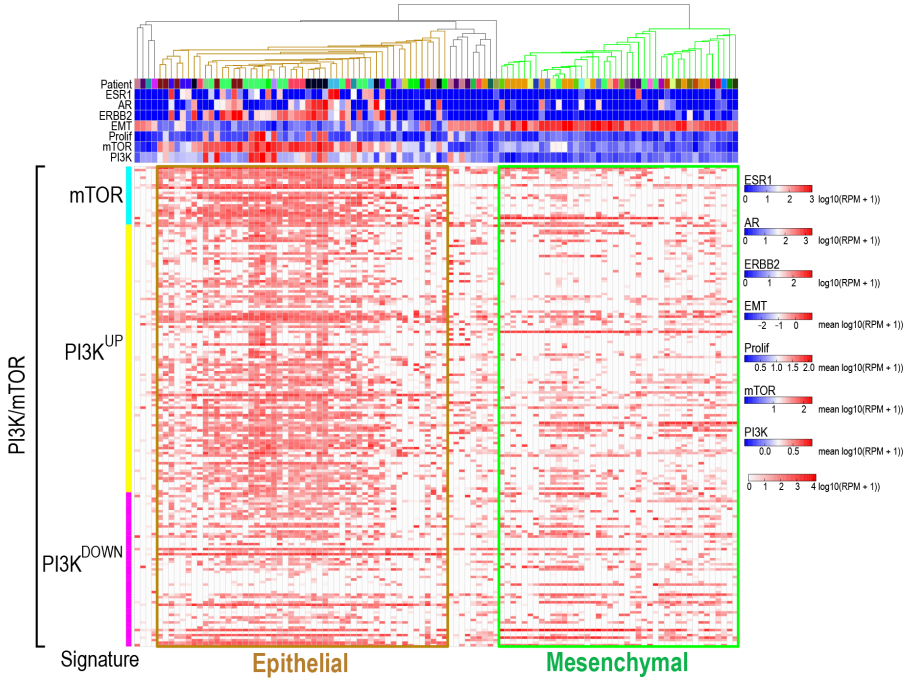

b)

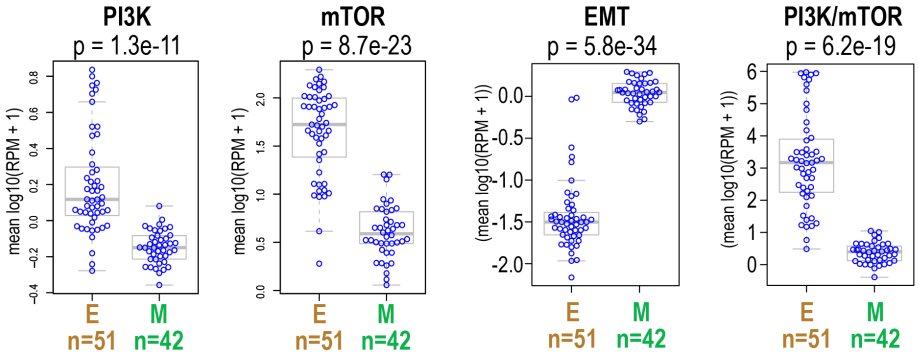

Supplementary Figure 14:

14a: Single cell RNA-Sequencing of 106 CTCs enriched from 33 metastatic breast cancer patients (Breast cancer dataset #2). Top dendrogram represents EMT signature-based hierarchical clustering of single CTCs represented in columns below. Top rows represent patient ID, and gene signature levels. Rows below represent individual transcript levels used for calculating mTOR and PI3K signatures.

14b: Based on the hierarchical clustering, epithelial and mesenchymal subsets of CTCs were selected and analyzed for PI3K and mTOR signatures. The plots show the level of the individual PI3K and mTOR signaling and combined PI3K/mTOR gene signatures in each individual CTCs enriched from breast cancer patients (dataset #2) harboring wild type or mutant PI3K. The p-values shown were calculated using the two-sided Welch t-test.

Supplementary Figure 15

Breast cancer CTC dataset 1

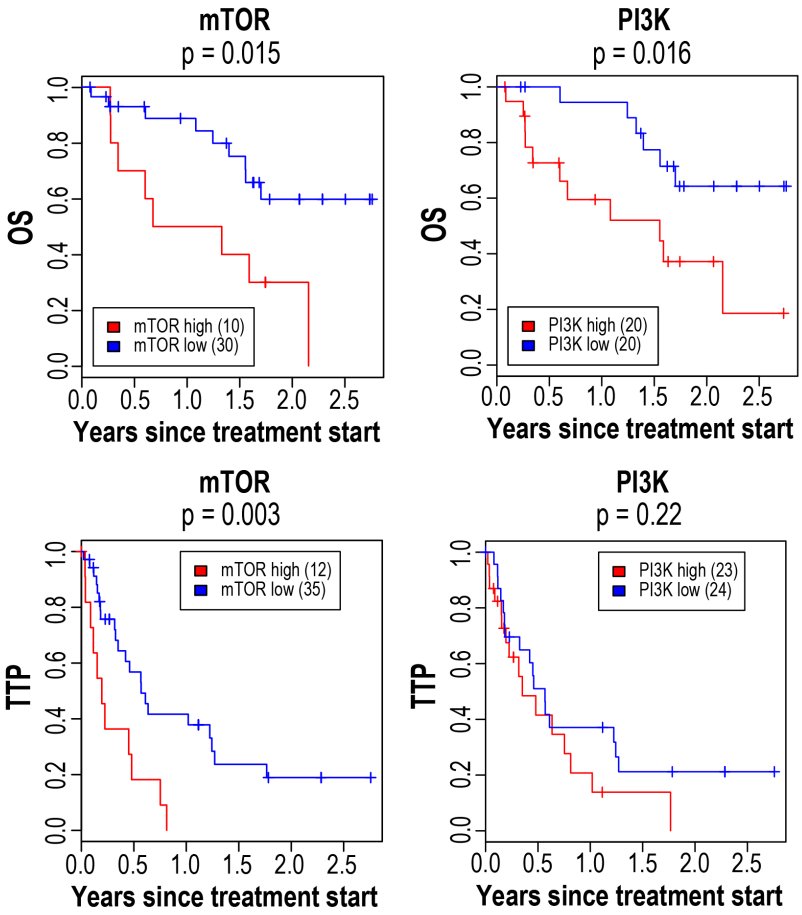

Supplementary Figure 15:

Kaplan-Meier analysis of overall survival (OS) and time to progression (TTP) on previous therapy for breast cancer patients (dataset #1, Supplementary Table 3) with high average PI3K and mTOR activity versus low average PI3K and mTOR activity. The high and low PI3K and mTOR subgroups were determined based on average PI3K and mTOR activity for each patient blood draw. P-value was calculated by log rank test.

Supplementary Figure 16

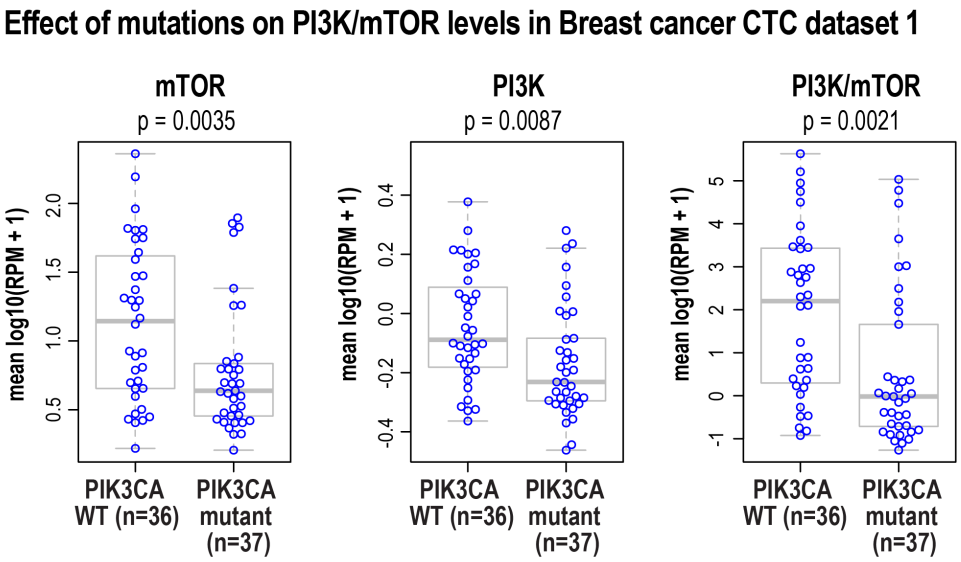

Supplementary Figure 16:

The plots show the level of the individual PI3K and mTOR signaling and combined PI3K/mTOR gene signatures in each individual CTCs enriched from breast cancer patients (dataset #2) harboring wild type or mutant PI3K. The p-values shown were calculated using the two-sided Welch t-test.

SUPPLEMENTARY METHODS:

FACS sorting

BD FACSAria II Cell Sorter was used to sort PC3 cells labeled with the N-Cadherin antibody (Clone 8C11, PE labeled, Biolegend). PE Mouse IgG1 (Biolegend) was used as isotype control. Gating strategy is shown in **Supplementary Fig. 10a**.

Cell Proliferation Assay

Proliferation was measured using CellTiter-Glo (Promega). Briefly, 2,000 cells were plated in each well of a 96-well plate in a volume of 100 µl growth medium at day 0. At indicated time points, 100 µl of CellTiter-Glo reagent was added into each well and measurements were done using a luminescence plate reader.

Western blot analysis

Cells were lysed in RIPA Buffer (cat# BP-115X) supplemented with Halt™ Protease inhibitor cocktail (Thermo Scientific cat# 78425) and passed through a needle to enhance lysis. Protein concentration was determined using Pierce™ BCA Protein Assay Kit (Thermo Scientific cat# 23227). Protein lysates, 15 µg per sample, were separated on SDS/4-15% polyacrylamide gels (Bio-Rad) and transferred onto nitrocellulose membranes (Invitrogen). After blocking with 5% BSA buffer for 1 hour at room temperature, membranes were incubated with primary antibodies overnight at 4°C and followed with the relevant HRP-conjugated secondary antibodies against rabbit and mouse (Cell Signaling Technology Cat# 7074, RRID:AB_2099233; Cat# 7076,

RRID:AB_330924) and visualized using Clarity Western ECL Substrate (BIORAD) and G box (Syngene). ß-actin was used as a loading control. The following primary antibodies (details listed in Supplementary Table 1) were used for western blotting: c-Met (Cell Signaling; 1:1000), pS6 (Fluidigm; 1:1000), Total S6 (Cell Signaling; 1:1000), p4EBP1 (Fluidigm; 1:500), Total 4EBP1 (Cell Signaling; 1:1000), pAKT308 (Cell Signaling; 1:1000); pAKT473 (Fluidigm; 1:1000), Total Akt (Cell Signaling; 1:1000), ß-actin (Cell Signaling; 1:1000).

Clustering technique

SPADE clustering was implemented by Cytobank. We performed SPADE with 40 nodes and 1% downsampling, and clustered using the following epitope levels: EpCAM, EGFR, c-Met, HER3, HER2, CD44, pS6, p4EBP1, pAkt308, p-p38, pStat3, pErk, p-p90RSK.

Analysis of single cell 10X RNA-Sequencing data from patient-derived prostate cancers

Single cell RNA-seq data of 13 prostate tumor samples (12 patients: 12 primary tumors and 1 lymph node metastasis) sequenced with 10x Genomics were downloaded from the NCBI Gene Expression Omnibus (GEO) (RRID:SCR_005012) accession GSE141445(2). Data were imported into R (v4.0.3) for preprocessing and analysis. Quality control was performed as described in (2) with a more stringent cutoff that cells with less than 500 genes expressed were filtered out and genes expressed in less than 10 cells were excluded. Downstream analysis and visualization were performed using Seurat (v4.0.3)(3,4). Major cell types were annotated using SingleR (v1.4.1)(5) using

the Human Primary Cell Atlas (HPCA) as reference(6). Copy number alterations (CNAs) of clusters of epithelial cells and a relatively large cluster annotated as tissue stem cells were inferred by inferCNV (v1.6.0, https://githubcom/broadinstitute/inferCNV) using lymphocytes as "normal" control. The detection of CNAs in these cells indicates the malignancy of these cells, and these malignant cells were included for assigning epithelial and mesenchymal lineages as described earlier in the analysis of single cell CTC prostate cancer cells, followed by the measurement and comparison of PI3K/mTOR activity.

Statistical analysis:

Median levels of individual epitopes from *in vitro* treatment analysis were compared using multiple t-tests, corrected using Bonferroni-Dunn method ($p<0.05$, number of tests: 200). Median levels of epitopes in graft experiments were compared using multiple t-tests with FDR correction ($q<0.1$) corrected for multiple comparisons using two-stage Benjamini, Krieger and Yekutieli correction. Medians levels of epitopes in BEZ235 or GDC0941 *in vivo* treatment experiments were compared using multiple t-tests with FDR correction corrected for multiple comparisons using two-stage Benjamini, Krieger and Yekutieli correction ($q<0.1$). For statistics of single cell PI3K/mTOR indices, samples with more than 5,500 cells were down sampled to avoid cells from a single animal to be overrepresented in the result. The down sampling was performed by select random sample function of JMP. The PI3K/mTOR indices were compared by Mann-Whitney test ($p<0.001$) and was accepted significant only when medians values of PI3K/mTOR of all cells from each animal showed identical directional change.

SUPPLEMENTARY REFERENCES:

1. Otsu. Threshold Selection Method from Gray-Level Histograms. IEEE Transactions on Systems, Man, and Cybernetics 1979;9:62-6
2. Chen S, Zhu G, Yang Y, Wang F, Xiao YT, Zhang N*, et al.* Single-cell analysis reveals transcriptomic remodellings in distinct cell types that contribute to human prostate cancer progression. Nat Cell Biol 2021;23:87-98
3. Hao Y, Hao S, Andersen-Nissen E, Mauck WM, 3rd, Zheng S, Butler A*, et al.* Integrated analysis of multimodal single-cell data. 2021;184:3573-87 e29
4. Satija R, Farrell JA, Gennert D, Schier AF, Regev A. Spatial reconstruction of single-cell gene expression data. Nat Biotechnol 2015;33:495-502
5. Aran D, Looney AP, Liu L, Wu E, Fong V, Hsu A*, et al.* Reference-based analysis of lung single-cell sequencing reveals a transitional profibrotic macrophage. Nat Immunol 2019;20:163-72
6. Mabbott NA, Baillie JK, Brown H, Freeman TC, Hume DA. An expression atlas of human primary cells: inference of gene function from coexpression networks. BMC Genomics 2013;14:632